ACS Combinatorial Science

Research Article

pubs.acs.org/acscombsci

Preparation of 24 Ternary Thin Film Materials Libraries on a Single Substrate in One Experiment for Irreversible High-Throughput Studies

Pio John S. Buenconsejo,* Alexander Siegel, Alan Savan, Sigurd Thienhaus, and Alfred Ludwig*

Institute for Materials, Ruhr-Universität Bochum, 44780 Bochum, Germany

Supporting Information

ABSTRACT: For different areas of combinatorial materials science, it is desirable to have multiple materials libraries: especially for irreversible high-throughput studies, like, for example, corrosion resistance testing in different media or annealing of complete materials libraries at different temperatures. Therefore a new combinatorial sputter-deposition process was developed which yields 24 materials libraries in one experiment on a single substrate. It is discussed with the example of 24 Ti–Ni–Ag materials libraries. They are divided based on the composition coverage and orientation of composition gradient into two sets of 12 nearly identical materials libraries. Each materials library covers at least 30–40% of the complete ternary composition range. An acid etch test in buffered-HF solution was performed, illustrating the feasibility of our approach for destructive materials characterization. The results revealed that within the composition range of Ni < 30 at.%, the films were severely etched. The composition range which shows reversible martensitic transformations was confirmed to be outside this region. The high output of the present method makes it attractive for combinatorial studies requiring multiple materials libraries.

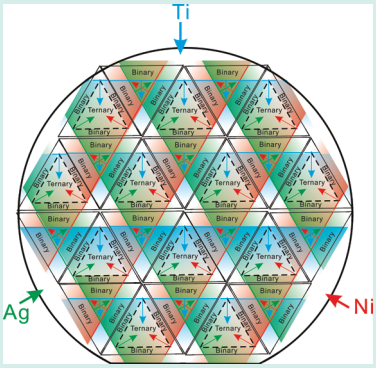

KEYWORDS: *combinatorial materials science, shape memory alloys, thin films, etching, Ti–Ni–Ag*

INTRODUCTION

One of the key concepts of combinatorial materials science (CMS) is to cover large compositional parameter spaces by fabricating materials libraries that consist of a large amount of well-defined and highly comparable samples. Using these materials libraries, high-throughput experimentations are carried out to "screen" for specific properties, for example, phase transformation properties in (ferromagnetic) shape memory alloys, electronic/magnetic properties in semiconductors, or hydrogen production and storage properties of alloys. The CMS methodology can speed up the process of identification or discovery of novel materials with promising properties for applications. In fact this method has been successfully applied to a wide range of materials discovery and development efforts in various fields of science and technology,[1−13] such as semiconductors, magnetic materials, shape memory alloys, and battery materials.

CMS methodologies are still continually being further developed to allow for more efficient studies of new materials. An important challenge is how to effectively fabricate in a short time, sets of identical materials libraries, which are then used to study irreversible processes, such as influences of postdeposition processing or reactive environments on the materials. The preparation of a complete ternary system on a substrate frequently starts with depositing the desired elements by sputter-deposition methods (typically wedge-type multilayer depositions[13]). The as-deposited materials library is then further processed: for example, by annealing to change the state of the material through alloying, crystallization, phase precipitation, etc. Finally, the materials libraries are characterized by adequate high-throughput screening methods, for example, resistivity and phase constitution.

However, in most scientific investigations the variation of postdeposition processing parameters is necessary, such as annealing at various temperatures and times, or exposure to different reactive environments. If a complete materials library is annealed at one temperature it is usually not any more usable for a further annealing experiment. A good example is the identification of irreversible phase transformation temperatures. Also there are cases where the high-throughput characterization is a destructive process, that is, corrosion or acid-etch tests, and oxidation experiments in different media. If a complete materials library is used for testing of the corrosion resistance, it is necessary to have a complete materials library for each test at different conditions (e.g., etching medium, concentration, time, etc.) Using the conventional technique of sequentially depositing single materials libraries would then be cumbersome, that is, it would require a lot of time, resources and efforts to prepare multiple materials libraries. For these purposes, the simultaneous preparation of multiple materials libraries is necessary. One approach for the preparation of multiple libraries in a single experiment was reported by Dahn

Received: August 2, 2011
Revised: October 28, 2011
Published: November 30, 2011

et al.[11,12] They used a special turntable with shadow-masking sputter approach which is capable of simultaneously fabricating 5 ternary or quaternary materials libraries.

Here, we report on the development of a multilayer sputter deposition process which yields multiple (24 in this example) ternary materials libraries on a single 4 in. SiO_2/Si wafer substrate. Issues regarding the preparation of the materials libraries are discussed. Since we use shape memory alloys (SMA) as an example system, the phase transformation properties are characterized and the feasibility of using these small materials libraries for acid etch testing is presented. This is related to the applicability of SMA in harsh environments.

RESULTS AND DISCUSSION

TiNi-based SMA undergo reversible martensitic transformations that lead to the shape memory effect and superelastic behavior.[14] These functions have made them attractive for actuator and biomedical applications. The Ti−Ni−Ag SMA system was chosen for this study, as the addition of Ag to TiNi could be beneficial for the development of SMA devices with antibacterial functions.[15−17] For such biomedical experiments a multitude of identical materials libraries are necessary to increase statistical confidence of the test results. Furthermore the materials need to be resistant to harsh environments.

Figure 1a illustrates the sputter-deposition scheme for the preparation of 24 materials libraries on one 4 in. diameter substrate using the example system Ti−Ni−Ag. It is a schematic top view showing the position of the composition or thickness wedges for each element, where Ti is blue, Ni is red, and Ag is green. For each element there are four wedges indicated by colored arrows and they are deposited using a pair of moveable shutters to progressively mask and expose the substrate to the respective elemental targets. For an animated version of the wedge-type deposition process please refer to Supporting Information. As shown in Figure 1b, a sputter target is facing the substrate and between them computer-controlled moveable masking shutters are present. The sputter targets are fixed on magnetron cathodes attached to a moveable linear arm, above the substrate. The position of the arm is moved horizontally with respect to the stationary substrate, until the desired element to be deposited is directly facing the substrate. Close to the target is a source shutter which opens when the material is deposited. The target to substrate distance is about 132 mm; between them computer-controlled moveable masking shutters are present. They are kept close to the surface of the substrate in order to maximize their masking effect. To avoid damaging the substrate surface during shutter movement a clearance gap of about 3 mm is maintained between the substrate surface and the movable shutter blades during the deposition. The masking shutters come in pairs (shutter 1 and shutter 2). First they move to the desired wedge starting position and the gap between them is initially closed. During the wedge deposition, shutter 2 moves at a constant speed (i.e., 1 mm/sec) until a gap of 15 mm is opened, whereas shutter 1 is fixed, i.e. shutter 2 produces the gradient, while shutter 1 masks the area not to be deposited. After deposition of the first wedge, the source shutter is closed while waiting for the masking shutters to position for deposition of the second wedge. The four wedges are deposited using this sequence, resulting theoretically in an ideal wedge shape. The four wedges are separated from each other by a gap of 7 mm, which is intended to isolate the triangular materials libraries from each other. The wedge gradients are positioned as follows: Ti

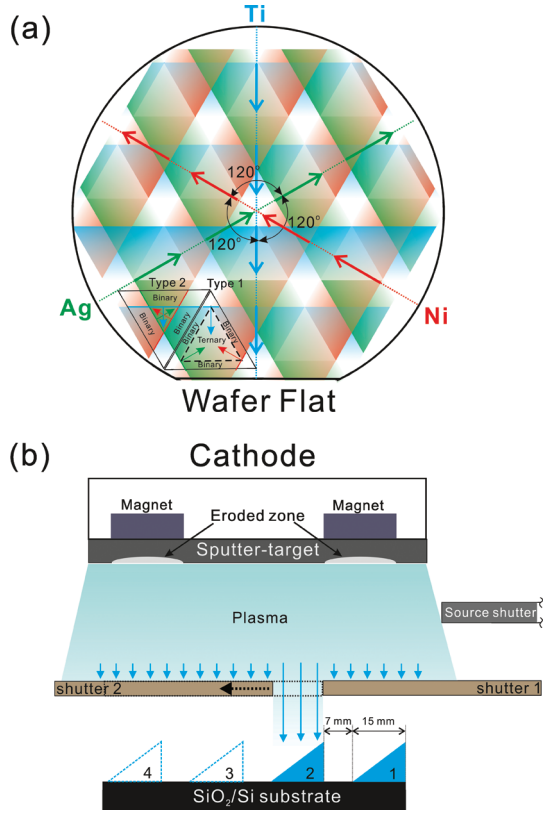

Figure 1. (a) Sputter-deposition scheme for multiple ternary materials libraries deposited on a single substrate shown for the example system Ti−Ni−Ag. The colored arrows indicate the directions of the thickness gradients, whereas circle arrows indicate the substrate rotation. The two types of ternary materials libraries are shown in the lower left of the wafer and the binary and ternary composition areas are indicated. (b) Schematic of wedge deposition using two movable shutters: shutter 1 defines the area of deposition, whereas shutter 2 creates the wedge shape of the deposited material.

wedges (blue) are perpendicular to the wafer flat, whereas Ni (red) and Ag (green) wedges are deposited after every substrate rotation of 120° about the center of the substrate. The whole process is repeated creating a multilayer of $(Ti/Ni/Ag)_n$ composition wedges with n repetitions. From this deposition scheme, two types of materials libraries are obtained shown as black triangles in Figure 1a. Type 1 (triangle pointing up) consists of composition gradients that start from the corners and end on the opposing side. The ternary composition mixture is indicated by a dashed triangle. Furthermore binary composition mixtures are found at the sides. This type of library should ideally cover the complete ternary composition space. Type 2 is an inverted triangle, where the region of ternary compositions is found in a small region at the center, again with binary composition mixtures along the sides. The composition space covered for this type is incomplete due to overlapping of the composition gradients. As shown in Figure 1a for the type 2 triangle, the thickest end of the Ti gradient overlaps midway along the Ag and Ni gradients on the right and left sides, respectively.

Figure 2 shows element-specific composition contour maps from the whole wafer obtained by automated EDX analysis with a measurement point grid of 4.5 mm by 4.5 mm. The $X-Y$ axes correspond to relative position where the center of the substrate is the origin. For each element, the intended 4

dx.doi.org/10.1021/co2001263 | ACS Comb. Sci. 2012, 14, 25−30

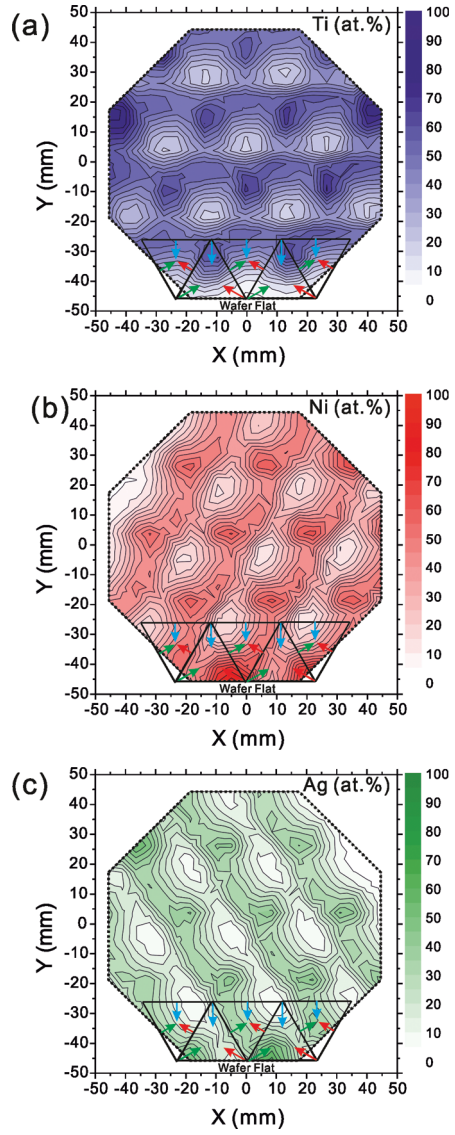

Figure 2. Element-specific composition contour maps obtained by automated EDX analysis of the whole wafer (measurement grid of 4.5 mm by 4.5 mm) for (a) Ti, (b) Ni, and (c) Ag.

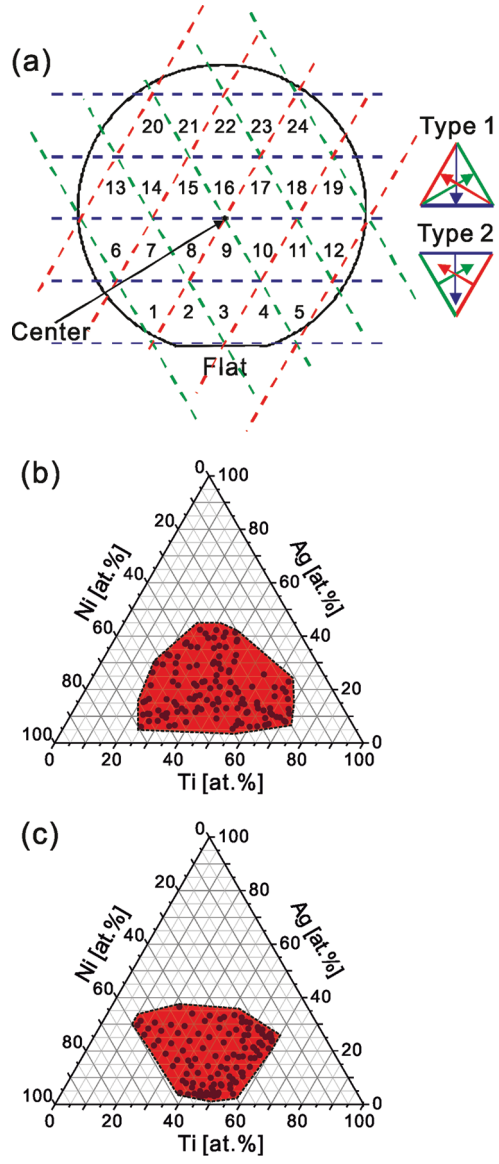

Figure 3. (a) Schematic of wafer-dicing based on the actual EDX results shown in Figure 2. Two types of triangles were obtained (type 1 and type 2). The results of EDX mappings for (b) type 1 and (c) type 2 materials libraries are plotted in ternary composition diagrams.

composition wedges are confirmed by the measured data. For the Ti wedges (shown as blue, Figure 2a) the composition gradients are perpendicular to the wafer flat. The Ni wedges (shown as red, Figure 2b) and Ag wedges (shown as green, Figure 2c) are each positioned after 120° rotations relative to the center of the substrate. Black triangles are shown to indicate the ternary materials libraries and the colored arrows inside it indicate the directions of the respective composition gradients. Corresponding to Figure 1, two types of triangular materials libraries are confirmed.

On the basis of the deposition scheme shown in Figure 1, wafer-dicing along the dashed lines was carried out, resulting in 24 separate triangular ternary materials libraries as shown in Figure 3a. The colored dashed lines indicate the boundary of the composition wedge for each element (Ti, blue; Ni, red; Ag, green). They are separated into two sets of 12 identical libraries according to the orientation of the triangular library. EDX mapping with a measurement point grid of 1.5 mm by 1.5 mm was carried out for both types of libraries. Representative results are plotted in composition diagrams for type 1 (Figure 3b) and type 2 (Figure 3c). The covered composition is shaded in red and comprises at least 30−40% of the ternary composition space. The expected binary mixtures along the sides of the triangular materials library (shown in Figure 1) were not found, but instead the ternary mixtures were found. The reason for this is explained in Figure 4 and below.

Figure 4a shows a 3D view of the Ti composition wedges along a line that passes through the center of the substrate and perpendicular to the wafer flat orientation. The wedge height is given in at. % since it is based on the EDX data. Each wedge was deposited in sequence according to the number label. The arrows point to the direction that the computer-controlled shutters moved during deposition to create the composition wedge. According to the proposed deposition scheme, the gaps between the wedges should be of zero thickness, (i.e., 0 at. % Ti in the EDX measurement), but instead, they were coated. The material deposited in the gap area amounts to 15−30 at. % of the respective element. The coated gaps result in the formation

dx.doi.org/10.1021/co2001263 | ACS Comb. Sci. 2012, 14, 25−30

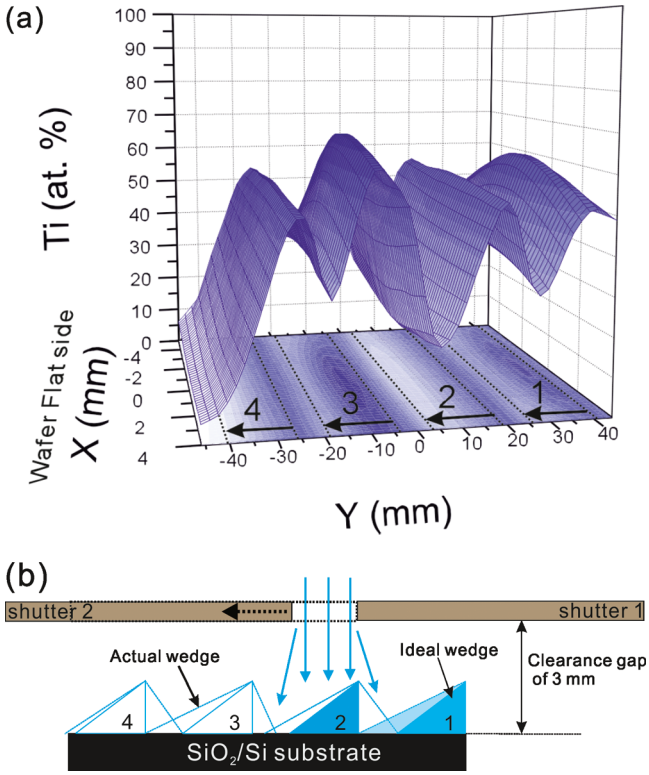

Figure 4. (a) A 3-D view of four Ti composition wedges along a line that passes through the center of the substrate and perpendicular to the wafer flat edge. The numbers correspond to the sequence that the wedges were deposited. (b) Schematic difference in the wedge profile between ideal wedge and the actual wedge.

of an additional unintended composition gradient, which runs opposite to the intended composition gradient. This unintended composition gradient is steeper compared to the intended composition gradient.

As discussed in Figure 1b, the shutter-mask deposition approach employed in this study should lead to the formation of ideal wedges. However as revealed in the EDX results, the actual wedge deposited is not identical to the ideal wedge (Figure 4b). For a zero clearance between shutters and substrate, the sputtered atoms that arrive at the substrate would be only proportional to the area exposed by the masking shutters. Due to the clearance gap of 3 mm between the substrate and the masking shutters, the sputtered atoms actually are deposited also under the shutters. These sputtered atoms arrive from directions not perpendicular to the target surface, due to the sputtering process and gas phase scattering. This explains how the intended gaps between the wedges disappear. Similar effects were also observed for the case of Ni and Ag composition wedges. The combination of the above effects for each of the elemental wedges results in the incomplete coverage of the ternary composition diagram and the disappearance of the binary mixtures along the sides of the triangular libraries.

Although a complete coverage of the ternary composition diagram was not achieved, the resulting materials libraries cover a substantial amount (30–40%) of the Ti–Ni–Ag alloy system. The main problem was the deposition under the masking shutters. In order to minimize this effect, a lift-off photoresist mask or a micromachined Si mask can be placed directly on the substrate surface. This would eliminate the unintended coating of the gaps between the wedges. Furthermore, by using comparable deposition rates for all elements to be deposited it is easier to create composition wedges with comparable wedge thickness gradients. This will help improve the distribution of composition and achieve complete composition coverage. As these optimization steps require further extensive experimentation they are beyond the scope of this paper. Instead, the feasibility of using the obtained triangular materials libraries for combinatorial studies where they are subjected to subsequent irreversible processing and testing were carried out.

Ti–Ni–Ag materials libraries were subjected to acid-etch testing using a buffered HF solution (NH_4F–HF, 35–6% by volume), which is an important etchant in Si-based microfabrication process, that is used for the removal of oxide layers. Figure 5 shows two materials libraries etched for 30 and 120 s,

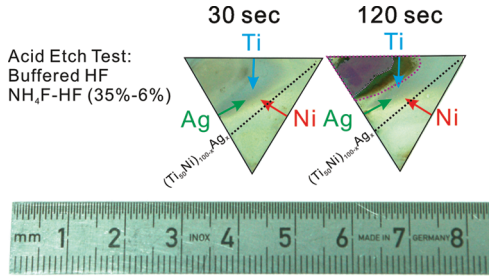

Figure 5. Photos of Ti–Ni–Ag materials libraries after acid etch test in a buffered HF solution (NH_4F–HF, 35–6%) at different etching times. The two separate samples began as two identical materials libraries. The arrows indicate the direction of the composition gradient from high to low content for each element. The dashed line corresponds to the $(Ti_{50}Ni)_{100-x}Ag_x$ composition. Scale is shown for reference.

respectively. The materials library etched for 30 s shows no distinguishable changes on the surface compared to the as-deposited materials library. The surface features observed are attributed to the composition gradients. However, the materials library etched for 120 s shows significant changes: obviously, a large portion of the materials library was etched away. Comparing this with the EDX results, the etched region was found to be strongly dependent on the Ni content. This region corresponds to the composition boundary of Ni < 30 at.%.

It is noted that residual strain is present in the film due to the difference of thermal expansion between the film and the substrate. This may affect the etching of the film, but in the present study it is considered that it does not strongly affect the etching process more than the influence of the composition. This is obvious from the strong composition dependence of the etch test results.

Previously it was reported that due to the limited solubility of Ag in the phase transforming TiNi SMA, the ternary system behaves like a pseudobinary $(Ti_{50}Ni)_{100-x}Ag_x$.[15,16] So for compositions in Ti–Ni–Ag having a Ti:Ni ratio close to 50:50, they are expected to exhibit reversible phase transformation similar to binary $Ti_{50}Ni$ SMA.[14] This composition range is indicated in Figure 5. For example the sample $Ti_{50.8}Ni_{44.8}Ag_{4.4}$ (equivalent to $(Ti_{53.1}Ni)_{95.6}Ag_{4.4}$) exhibits a reversible phase transformation as shown in the resistance–temperature, $R(T)$, curve in Figure 6a. This is a typical $R(T)$ curve of the B2-R phase transformation characterized by a small transformation hysteresis (ΔT = 3.1 K) and considered important for high-speed microactuator applications. Compositions lying far from the transforming region, such as shown in

dx.doi.org/10.1021/co2001263 | ACS Comb. Sci. 2012, 14, 25–30

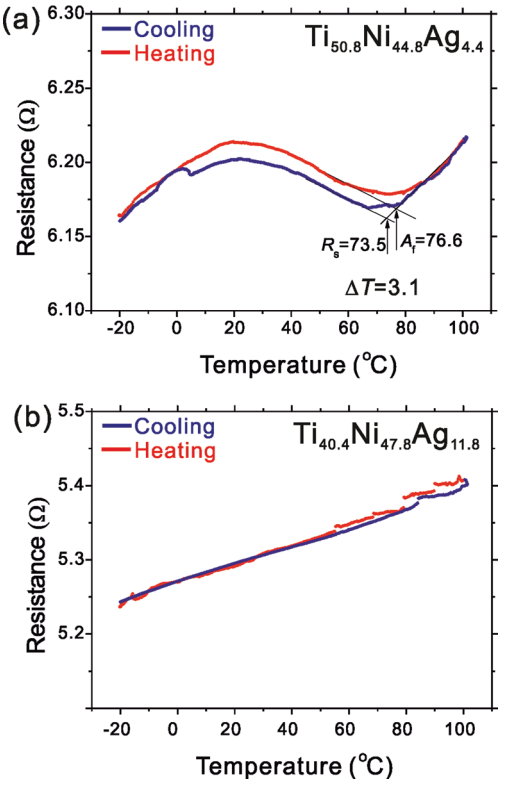

Figure 6. Typical examples of resistance-temperature curves confirmed in Ti−Ni−Ag materials libraries. (a) B2-R reversible phase transformation, where R_s and A_f are the R phase start transformation and reverse transformation finish temperatures, respectively. The thermal hysteresis (ΔT) is the difference between them. (b) Nontransforming composition exhibiting a linear resistance-temperature behavior.

Figure 6b, exhibit typical $R(T)$ curves, which are characteristic for normal metals (linear dependence of resistance with temperature).

In summary, 24 Ti−Ni−Ag materials libraries were successfully prepared on a 4-in. SiO_2/Si substrate in a single experiment. The feasibility of using them for acid etch testing was confirmed, revealing a composition range severely attacked by buffered HF solution. Reversible phase transformation was confirmed to be outside this etched region. In the future, we envisage developing and optimizing the presented concept methodology to perform more efficient combinatorial studies requiring multiple libraries, that is, corrosion performance or biocompatibility of novel alloys.

EXPERIMENTAL PROCEDURES

A combinatorial sputter-deposition system (DCA, Finland) equipped with multiple cathode positions and movable masking shutters was used to deposit the materials libraries.[13] Prior to deposition, a base vacuum pressure of less than 1.0×10^{-7} mTorr was attained. For the deposition process the following parameters were constant: Ar pressure at 5 mTorr, substrate to target distance of 132 mm, and substrate temperature at 25 °C. Multilayer composition wedges of pure Ti, Ni and Ag were deposited on a 4-in. SiO_2/Si wafer substrate from high-purity (>99.9 at.%) elemental sputter targets. The SiO_2 layer (stable up to about 850 °C) acts as a diffusion barrier between the bulk Si substrate and the thin films. A single deposition loop comprising of Ti/Ni/Ag layers were deposited with nominal thickness gradients given in Table 1. These were computed from the measured sputter-rate of each element. In total, 20 deposition loops were made. The deposition scheme is shown in Figure 1 and explained in the main text section above.

Table 1. Sputter-Deposition Parameters

Sputter-target	Power (W)	Sputter-rate (nm/sec)	Nominal thickness gradient (nm)
Ti	210 W, DC.	0.27	0−4.05
Ni	75 W, DC.	0.16	0−2.4
Ag	100 W, R.F.	0.037	0−0.6

After deposition the whole wafer, that is, all 24 materials libraries, was annealed at 500 °C for 1 h under high vacuum and left to cool down to room temperature inside the chamber. The composition mapping was performed in a scanning electron microscope (SEM, JEOL JSM 5800LV) equipped with an energy dispersive X-ray (EDX) spectroscopy system. The composition mapping at various measurement grids (4.5 mm × 4.5 mm for whole wafer mapping, 1.5 mm × 1.5 mm for single ternary library mapping) was carried out. The composition analysis was performed using an Oxford INCA 250 system consisting of the INCA X-act EDX detector and INCA-EDX software package. The measurement conditions were as follows: accelerating voltage = 20 kV; working distance = 10 mm; magnification = 600 (4.5 mm × 4.5 mm grid) and 1000 (1.5 mm × 1.5 mm grid). In the INCA software "Quant optimization" was performed (pure Co used as a Quant Optimization Element), to ensure that beam current fluctuations and temperature changes do not affect the quantitative analysis of elemental composition in the film The measured EDX spectra consist of contributions from the sample (Ti−Ni−Ag) and the substrate (SiO_2/Si). The contribution from the substrate was removed by normalizing the measured composition with respect to Ti, Ni and Ag only. The wafer was then diced to physically separate the 24 libraries. The phase transformation properties were characterized by four-point probe electrical resistance measurement during thermal cycling (heating and cooling rate of 5 K min^{-1}) between −20 and 100 °C. Acid etch testing was performed by immersion in a buffered HF (NH_4F−HF, 35−6% volume ratio) solution.

ASSOCIATED CONTENT

Supporting Information

A video animation of wedge-type sputter-deposition process of preparing ternary alloys system thin film materials libraries is available online. This material is available free of charge via the Internet at http://pubs.acs.org.

AUTHOR INFORMATION

Corresponding Author

*E-mail: pio.buenconsejo@rub.de (P.J.S.B.); alfred.ludwig@rub.de (A.L.).

Author Contributions

P.J.B. and A.L. conceived, designed, and conducted the experiments. A. Siegel, A. Savan, and S.T. setup the experiment test-stand and provided support during sample preparation and manuscript preparation.

Funding

This research was supported by the German Research Foundation (DFG) within the collaborative research center "SFB-459".

■ ACKNOWLEDGMENTS

The authors thank Kornelia Strieso for technical support during the acid-etch experiments. The video animation was made by Dario Grochla using blender animation program (http://www.blender.org).

■ REFERENCES

(1) Xiang, X.-D.; Sun, X.; Briceho, G.; Lou, Y.; Wang, K. A.; Chang, H.; Wallace-Freedman, W. G.; Chen, S.-W.; Schultz, P. G. A combinatorial approach to materials discovery. *Science* **1995**, *268*, 1738−1740.

(2) van Dover, R. B.; Schneemeyer, L. F.; Fleming, R. M. Discovery of a useful thin-film dielectric using a composition-spread approach. *Nature* **1998**, *392*, 162−164.

(3) Matsumoto, Y.; Murakami, M.; Shono, T.; Hasegawa, T.; Fukumura, T.; Kawasaki, M.; Ahmet, P.; Chikyow, T.; Koshihara, S.; Koinuma, H. Room-temperature ferromagnetism in transparent transition metal-doped titanium dioxide. *Science* **2001**, *291*, 854−856.

(4) Takahashi, R.; Kubota, H.; Tanigawa, T.; Murakami, M.; Yamamoto, Y.; Matsumoto, Y.; Koinuma, H. Development of a new combinatorial mask for addressable ternary phase diagramming: application to rare earth doped phospors. *Appl. Surf. Sci.* **2004**, *223*, 249−252.

(5) Ludwig, A. Combinatorial fabrication of magnetic multilayer films. *Appl. Surf. Sci.* **2004**, *223*, 78−83.

(6) Cui, J.; Chu, Y.; Famodu, O. O.; Furuya, Y.; Hatttrick-Simpers, J.; James, R. D.; Ludwig, A.; Thienhaus, S.; Wuttig, M.; Zhang, Z.; Takeuchi, I. Combinatorial search of thermoelastic shape memory alloys with extremely small hysteresis width. *Nat. Mater.* **2006**, *5*, 286−290.

(7) Zarnetta, R.; Takahash, R.; Srivastava, V.; Young, M. L.; Savan, A.; Furuya, Y.; Thienhaus, S.; Maass, B.; Rahim, M.; Frenzel, J.; Brunken, H.; Chu, Y. S.; James, R. D.; Takeuchi, I.; Eggeler, G.; Ludwig, A. Identification of quaternary shape memory alloys with near-zero thermal hysteresis and unprecedented functional stability. *Adv. Funct. Mater.* **2010**, *20*, 1917−1923.

(8) Hamann, S.; Gruner, M. E.; Irsen, S.; Buschbeck, J.; Bechtold, C.; Kock, I.; Mayr, S. G.; Savan, A.; Thienhaus, S.; Quandt, E.; Fähler, S.; Entel, P.; Ludwig, A. The ferromagnetic shape memory system Fe−Pd−Cu. *Acta Mat.* **2010**, *58*, 5949−5961.

(9) Buenconsejo, P. J. S.; Zarnetta, R.; König, D.; Savan, A.; Thienhaus, S.; Ludwig, A. A new prototype two-phase (TiNi)−(β-W) SMA system with tailorable thermal hysteresis. *Adv. Funct. Mater.* **2011**, *21*, 113−118.

(10) Buenconsejo, P. J. S.; Zarnetta, R.; Ludwig, A. The effects of grain size on the phase transformation properties of annealed (Ti/Ni/W) shape memory alloy multilayers. *Scr. Mater.* **2011**, *64*, 1047−1050.

(11) Dahn, J. R.; Trussler, S.; Hatchard, T. D.; Bonakdarpour, A.; Mueller-Neuhaus, J. R.; Hewitt, K. C.; Fleischauer, M. Economical sputtering system to produce large-size composition-spread libraries having linear and orthogonal stoichiometry variations. *Chem. Mater.* **2002**, *14*, 3519−3523.

(12) Chevrier, V.; Dahn, J. R. Production and visualization of quaternary combinatorial thin films. *Meas. Sci. Technol.* **2006**, *17*, 1399−1404.

(13) Ludwig, A.; Zarnetta, R.; Hamann, S.; Savan, A.; Thienhaus, S. Development of multifunctional thin films using high-throughput experimentation methods. *Int. J. Mater. Res.* **2008**, *99*, 1144−1149.

(14) Otsuka, K.; Ren, X. Physical metallurgy of Ti−Ni-based shape memory alloys. *Prog. Mater. Sci.* **2005**, *50*, 511.

(15) Zamponi, C.; Wuttig, M.; Quandt, E. Ni−Ti−Ag shape memory thin films. *Scr. Mater.* **2007**, *56*, 1075−1077.

(16) Oh, K.-T.; Joo, U.-H.; Park, G.-H.; Hwang, C.-J.; Kim, K.-N. Effect of silver addition on the properties of nickel-titanium alloys for dental application. *J. Biomed. Mater. Res. B. Appl. Biomater.* **2006**, *76B*, 306−314.

(17) Lansdown, A. B. Silver. I: Its antibacterial properties and mechanism of action. *J. Wound Care* **2002**, *11*, 125−130.